MORPHOMETRIC ANALYSIS AND COMPARISON OF MARTIAN LANDSLIDES AND LAYERED DEPOSITS OF IMPACT CRATER EJECTA BLANKETS. A. Pietrek[1] , J. Weis[1], S. Hergarten[1], G. Wulf[1] and T. Kenkmann[1], [1]Institute of Earth and Environmental Sciences - Geology, Albert-Ludwigs-University Freiburg, Germany (alexa.pietrek@geologie.uni-freiburg.de).

Introduction: Martian long runout landslides and the innermost, continuous deposits of particular double-layer (DLE) ejecta craters share characteristic features in their surficial morphologies. Among the most distinct are longitudinal ridges and grooves ("striations") and concentric troughs and ridges perpendicular to the striations, which appear to form related to the emplacement process. Most landslides in Valles Marineris show these features and it is a widespread feature for DLE craters. A terrestrial analog are strikingly similar longitudinal patterns observed on landslides deposited on a glacial substrate (e.g. Sherman landslide [1,2]). The formation mechanism of the longitudinal grooves and ridges in landslide deposits is poorly understood for both the Martian and terrestrial examples. They are proposed to form due to divergence during flow, either forming by widening and lateral spreading of the deposit [3] or longitudinal differences in flow velocity and lateral shear [4]. Lubrication at the base of the slide is judged prerequisite to enable the formation of longitudinal grooves [3] and is suggested to explain the high mobility of the landslides. Ice, (melt-)water, evaporites [3] or sheet-silicates [5] are discussed as possible basal lubricants. Lubrication at the base by ice or a melt-layer of water [6,7] is suggested to explain the fluidized morphology of layered crater deposits. [8] compared and modeled landslide and layered crater ejecta morphologies and concluded that emplacement by flow as basal glide fits best with the results. This study concentrates on determining how the distinct longitudinal lineation forms in both the landslide and ejecta deposits and whether a similar formation mechanism can be established.

Methods: The main study objects are the Coprates landslide (CL, 292.2°E, 11.8°S) in Valles Marineris and the inner layer of the DLE crater Steinheim (SC, 190.6°E, 54.5°N) in Arcadia Planitia. CTX DTMs were processed from stereo pairs using the NASA Ames Stereo Pipeline [9]. For Steinheim crater, HiRISE DTMs were provided by the NASA/JPL/University of Arizona. True thicknesses of all deposits were obtained by subtracting the underlying topography using ArcGIS. The substrate topographies were interpolated from the DTM raster values in the area surrounding the deposits with the Nearest Neighbor interpolation function of ArcMap.

Morphological comparison: CL is structured from rear to front in I) a chaotic, hummocky region formed partially of slump blocks (length *l* ~3-14 km), II) a wide, flat area of laterally spreading, continuous deposits, shaped by longitudinal striations and perpendicular troughs and ridges (*l* ~25-31 km) (Fig.1). The inner layer of SC can be structured into I) hummocky deposits at the base of the uplifted rim (*l* up to 1.7 km), II) a wide ring of continuous deposits marked by radial striations and concentric ridges and troughs (*l* ~7 km) and III) a visibly thickened, bulky zone (*l* ~1-1.7 km) [7]. Exemplary profiles perpendicular to the striations (Fig.1) of both deposits show that the longitudinal ridges are distinctly V-shaped and have stepped slopes where smaller ridges formed on the flanks of large ridges. Width to height proportions are similar, although the dimensions of the striations of Steinheim crater are about half the dimension of the striations of Coprates Landslide (Fig. 1P2/ PS).

On CL, broad, longitudinal grooves of several hundred meter width generally can be easily traced from the rear of the slide to the front. On the deposits of SC, striations can seldomly be traced from rim to rampart. Striations starting at the rim usually level out before reaching the middle and are replaced by new longitudinal ridges and grooves. Those new striations are usually more pronounced and have a higher width. Lateral spreading (widening of the deposit with distance from the source) can either be accommodated by widening of longitudinal ridges or formation of new ridges. On CL, bands of parallel grooves can be identified, which often can be traced to the rear of the slide. When the deposit spreads or fans out laterally, those bands split and propagate into different directions, often preserving their width, with new longitudinal ridges and grooves forming in the interstitials ("forking", Fig. 1A). On SC, propagating striations accommodate lateral spreading by simultaniously increasing the width and forming new longitudinal ridges in the interstitials of already established ridges (Fig. 1B). Forking and widening of striations occurs evenly distributed on SC. On CL, both occurs heterogenously, probably a response to the much higher susceptibility of landslide deposits to be diverted by the underlying topography.

Morphometric analysis: For two distinct bands of prominent longitudinal ridges and grooves in CL, 7 Swath profiles [10] perpendicular to flow direction were taken for each band (Fig. 1A). Distances and height of longitudinal ridges and slope values were measured for each profile.

Preliminary results of the slope analysis of the ridges show that at the rear of the slide, slopes range between 2-10°, leveling out at the front to range between 2-5° (Fig. 1C/D) . Flanks tilting 2-5° are most abundant at all distances.

Conclusions and Outlook: Although the longitudinal ridges and grooves look very similar in morphology and profile, important differences arise at close study. Those differences include the behavior during lateral spreading (forking vs. widening of grooves), extent (spreading continuously over the whole deposit or being halfway replaced by new striations) and scale. The latter is mitigated by results from [11], suggesting the dimensions of longitudinal striations increase with crater diameter. The other might be dependent on emplacement velocity, geometry or mechanism, as well as target/material properties. More morphometric data will be collected, including those from other representative VM landslides and suitable DLE craters, to further investigate how closely longitudinal striations on landslides and crater deposits can be related.

References: [1] Shreve R.L. (1966) *Science, 154,* 1639-1643.[2] McSaveney M.J. (1978) in *Rockslides and Avalanches,* Elsevier, Amsterdam. [3] DeBlasio F.V. (2011) *Planet. Space Sci., 59,* 1384-1392. [4] McEwen (1989) *Geology, 17,* 1111-1114. [5] Watkins J.A. (2015) *Geology, 43,* 107-110. [6] Weiss D.K. and Head J.W. (2014) *Icarus, 233,* 131-146. [7] Wulf G. and Kenkmann T. (2015) *Maps, 50,* 173-203. [8] Barnouin-Jha O.S. et al. (2005) *JGR, 110,* E04010. [9] Moratto et al. (2010) *41th LPSC,* Abstract #2364. [10] Hergarten S. et al. (2014) *Earth Surf. Dyn., 2,* 97-104. [11] Boyce J.M. et al. (2014) *46th LPSC,* Abstract#10.

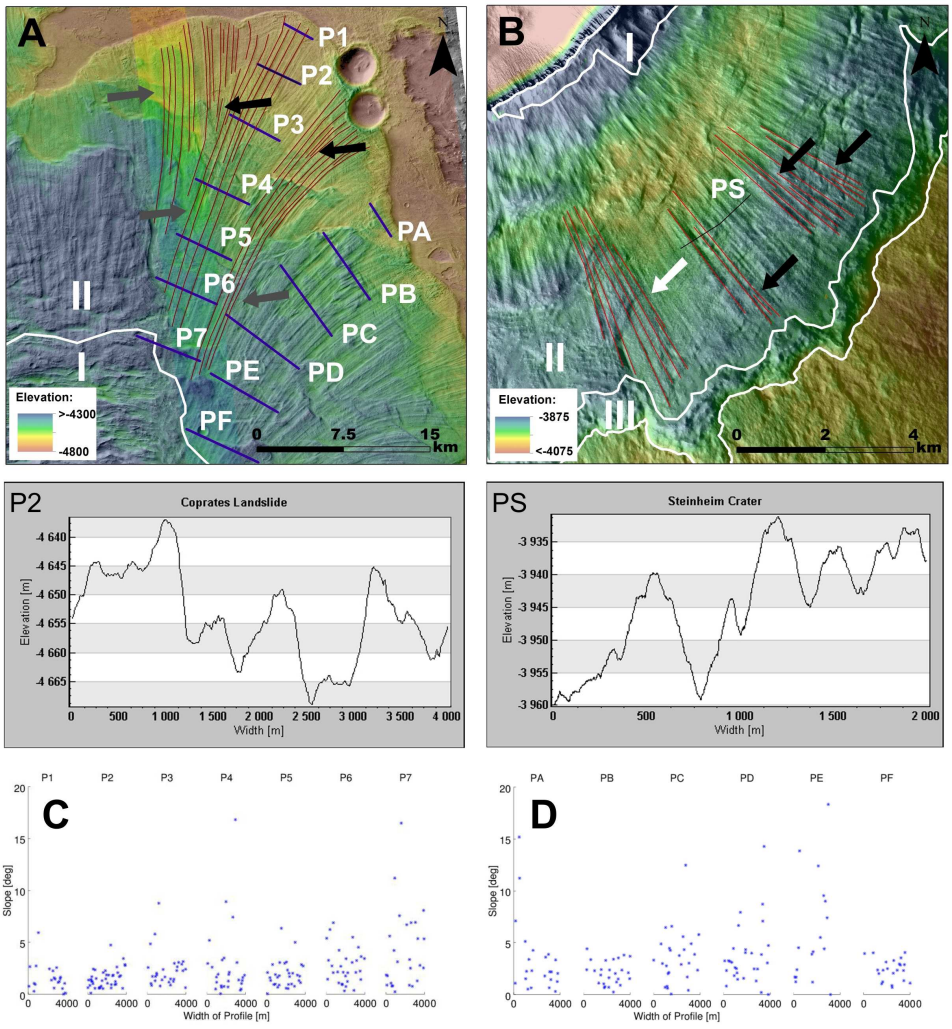

Figure 1: *A*) Coprates landslide. Black arrows point at forking of striations, grey arrows point at bands of parallel striations. Basis of the image is a Ctx mosaic, overlaid by two Ctx DTMs derived from Ctx stereo pairs.
P1-7 and PA-G are perpendicular profiles of CL, with the results of slope analysis in the bottom figures. *B*) SE area of the inner layer of Steinheim crater. Black arrows point at forking of striations, white arrows point at widening of striations as reaction to lateral spreading of the deposits. Basis of the image is a Ctx mosaic, overlaid by a DTM mosaic compiled from Ctx stereo pairs. *P2+PS*) Exemplary profiles of CL and SC, the position of the profiles is indicated in *A* and *B*.